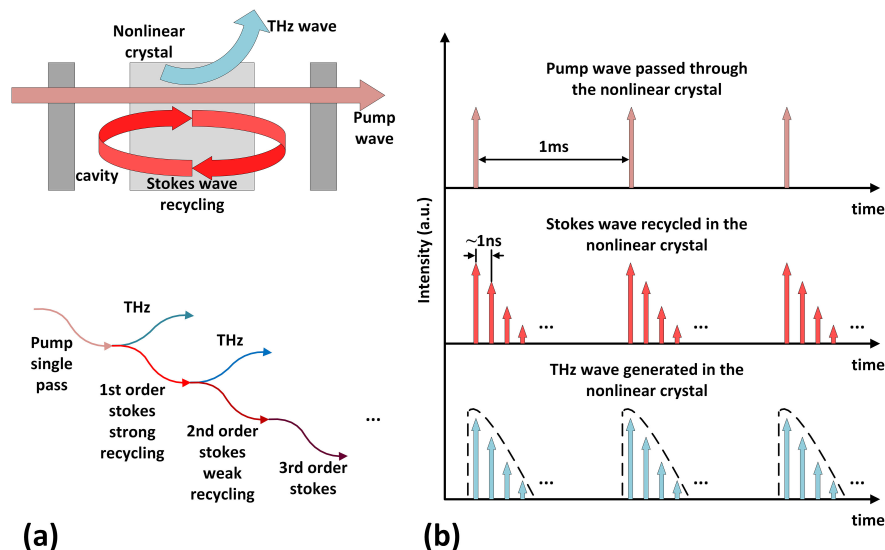


# Enhanced Terahertz Wave Generation via Stokes Wave Recycling in Non-Synchronously Picosecond Pulse Pumped Terahertz Source

Volume 11, Number 5, October 2019

Chao Yan  
Degang Xu  
Yuye Wang  
Zhaohua Wang  
Zhiyi Wei  
Longhuang Tang  
Yixin He  
Jining Li  
Kai Zhong  
Wei Shi  
Jianquan Yao



DOI: 10.1109/JPHOT.2019.2934488

# Enhanced Terahertz Wave Generation via Stokes Wave Recycling in Non-Synchronously Picosecond Pulse Pumped Terahertz Source

Chao Yan <sup>1,2</sup>, Degang Xu <sup>1,2</sup>, Yuye Wang <sup>1,2,3</sup>, Zhaohua Wang,<sup>4</sup>  
Zhiyi Wei,<sup>4</sup> Longhuang Tang <sup>1,2</sup>, Yixin He,<sup>1,2</sup> Jining Li <sup>1,2</sup>,  
Kai Zhong,<sup>1,2</sup> Wei Shi <sup>1,2</sup>, and Jianquan Yao<sup>1,2</sup>

<sup>1</sup>Institute of Laser and Optoelectronics, School of Precision Instruments and Optoelectronics Engineering, Tianjin University, Tianjin 300072, China

<sup>2</sup>Key Laboratory of Opto-electronic Information Technology (Ministry of Education), Tianjin University, Tianjin 300072, China

<sup>3</sup>Department of Neurosurgery and Key Laboratory of Neurotrauma, Southwest Hospital, Third Military Medical University, (Army Medical University), Chongqing 400038, China

<sup>4</sup>Beijing National Laboratory of Condensed Matter Physics, the Institute of Physics, Chinese Academy of Science, Beijing 100190, China

DOI:10.1109/JPHOT.2019.2934488

This work is licensed under a Creative Commons Attribution 4.0 License. For more information, see <https://creativecommons.org/licenses/by/4.0/>

Manuscript received July 23, 2019; accepted August 7, 2019. Date of publication August 12, 2019; date of current version September 13, 2019. This work was supported in part by the National Basic Research Program of China (973 Program) under Grant 2015CB755403, in part by the National Natural Science Foundation of China under Grants 61775160, 61771332, and 61675146, in part by the China Postdoctoral Science Foundation under Grant 2016M602954, in part by the Postdoctoral Science Foundation of Chongqing under Grant Xm2016021, and in part by the Joint Incubation Project of Southwest Hospital under Grants SWH2016LHJC04 and SWH2016LHJC01. Corresponding author: Yuye Wang (e-mail: yuyewang@tju.edu.cn).

**Abstract:** Enhanced terahertz wave generation via Stokes wave recycling in a non-synchronously picosecond pulse pump configuration has been demonstrated. It is theoretically analyzed that under the condition of high pump peak power density, the oscillation of the strong 1st order Stokes wave could benefit the higher order Stokes wave emission and terahertz wave generation. In the experiment, 5.71 times enhancement of terahertz wave generation was obtained via Stokes wave recycling in the non-synchronously picosecond pulse pumped terahertz parametric generator compared with the conventional single-pass terahertz parametric generation. The maximum terahertz wave average power was 61.7  $\mu$ W under the pump power of 20 W and the cavity length of 170 mm, while the maximum power conversion efficiency was  $3.085 \times 10^{-6}$ .

**Index Terms:** Terahertz radiation, Nonlinear optics, Raman scattering, Stimulated polariton scattering, Picosecond phenomena.

## 1. Introduction

The terahertz (THz) wave is attractive for more and more researchers because of its potential in a wide variety of applications in condensed matter physics, chemical engineering, life sciences and homeland security [1]–[2]. In the fields of the THz science and technology, high power THz sources is crucial concerns for researchers.

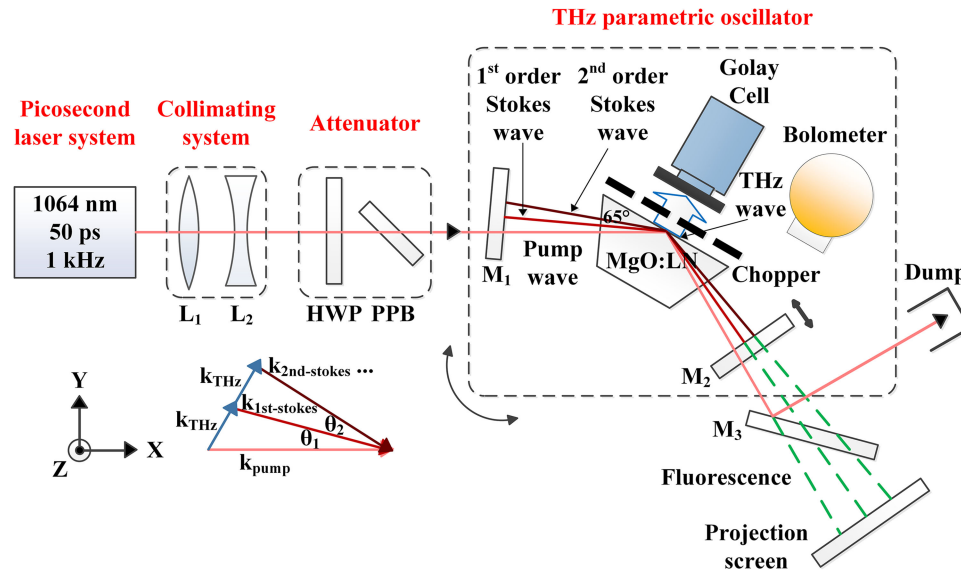


Fig. 1. The schematic diagram of the enhanced terahertz wave generation via Stokes wave recycling in non-synchronously picosecond pulse pumped terahertz source.

It is one of most promising methods to generate THz wave by stimulated polariton scattering (SPS) [3] in  $\text{LiNbO}_3$  ( $\text{MgO:LN}$ ) crystal. Terahertz parametric oscillator (TPO) based on SPS was firstly obtained by means of nanosecond (ns) pulse laser pumped configuration [4]–[6], and further developed by Kawase *et al.* [7]–[10]. After continuous improvement over decades [11]–[22], ns pumped TPO has already reached its limits owing to the harm of undesirable stimulated Brillouin scattering (SBS) effect. However, picosecond (ps) pulse pumped terahertz source could suppress the SBS effect and increase the conversion efficiency by about one order [23]. Therefore, ps pulse pumped terahertz sources have grown up recently, for example, injection-seeded terahertz parametric generators (is-TPG) with the maximum output of  $30 \mu\text{W}$  [24]–[31], and picosecond laser synchronously pumped TPOs (ps sync-TPO) with the maximum output of  $5.4 \mu\text{W}$  [32]–[34].

In this work, we proposed the enhanced THz wave generation via Stokes wave recycling based on a non-synchronously picosecond pulse pump configuration. Comparing with the conventional ps is-TPG and ps sync-TPO, this kind of configuration is simple and widely applicable. The oscillation of strong 1st order Stokes wave benefitted the higher order Stokes wave emission and terahertz wave generation. The experimental results show the maximum enhancement ratio of the THz power was 5.71 times compared with the conventional single-pass TPG configuration. When the pump power was 20 W and the cavity length was 170 mm, the maximum THz average power was  $61.7 \mu\text{W}$ , and the maximum power conversion efficiency was  $3.085 \times 10^{-6}$ . In addition, at this kind of maximum pump energy, broadband 1st order Stokes wave spectrum was observed over the 1069.08–1071.56 nm spectral region. We achieved a broad THz wave spectrum, ranging from 1.24 to 1.89 THz.

## 2. Experimental Details

The experimental setup is shown schematically in Fig. 1. The pump source was a diode-pumped all-solid-state picosecond amplifier system [35], which generated 1064.4 nm laser up to 20 W average power with pulse duration of 50 ps, the repetition rate of 1 kHz and a beam quality factor ( $M^2$ ) less than 2. A pair of lenses,  $L_1$  and  $L_2$ , made up the collimating system, which reduced the pump beam size to 3 mm. The variable optical attenuator was comprised of two parts: the half wave plate (HWP) and polarizing plate beam-splitter (PPB). A pair of plane-parallel mirrors  $M_1$  and  $M_2$

(Optical Coatings Japan Co.), which were both designed as anti-reflection from 1063 to 1064.7 nm ( $T > 98\%$ ) and high reflection from 1067 to 1100 nm (1067–1070 nm,  $R > 70\%$  & 1070–1078 nm,  $R > 90\%$  & 1078–1100 nm,  $R > 99\%$ ), made up the oscillating cavity. The nonlinear optical crystal was a 5 mol% MgO doped congruent LiNbO<sub>3</sub> (MgO:LN) crystal, with the shape of an isosceles trapezoid in the x–y plane. The longer base of the isosceles trapezoid was 40 mm, while the shorter base was 23.2 mm. The thickness of the MgO:LN crystal was 10 mm. The bottom angle of the isosceles trapezoid was 65°, which guaranteed that the pump wave and different orders Stokes wave were totally bounced at the surface of the MgO:LN crystal. This kind of configuration also allowed the THz wave to be emitted perpendicularly to the MgO:LN crystal surface, and had lower loss compared to Si-prism coupling configuration [36]. The polarization orientation of the pump wave and the Stokes wave were both parallel to the z-axis of the MgO:LN crystal. In addition, a rotating stage was utilized to assemble the oscillating cavity and the MgO:LN crystal. Considering that the time constant of Golay Cell detector (TYDEX, Inc.: GC-1P) is always larger than 10 ms and the optimum operation frequency is less than 50 Hz, the emitted THz radiation was chopped with an optical chopper (Stanford Research Systems: SR540) at a frequency of 10 Hz (50% duty cycle) and measured by the Golay cell. The Golay cell detector was calibrated by Tydex Inc., and the optical responsivity of the detector at the repetition rate of 10 Hz was 86.95 kV/W. In the experiment, the transmittance-calibrated black polyethylene (PE) sheet, which could exclude the direct injection of the intense pump and Stokes wave into the detector, was used as the THz wave low-pass filter. In addition, the black PE sheet was also treated as the THz wave attenuator to avoid the detector's saturation. In order to measure the THz pulse train with 1 kHz repetition rate, the 4K-Silicon bolometer (IRLabs: #3233) was utilized in the experiment, considering its time constant of about 1 ms. The spectral content of the Stokes wave was monitored using a calibrated optical spectrum analyzer (Yokogawa: AQ6370C). The THz wave frequency was inferred from the frequency difference of the fundamental and Stokes wavelengths.

### 3. Results and Discussion

In traditional terahertz parametric oscillator (TPO), the pump pulse duration is usually several nanoseconds, and the length of the pump wave train is about several meters. Under this condition, the oscillating Stokes wave could interact with the pump wave and generated narrowband THz wave. Other kinds of picosecond (ps) laser pumped TPOs usually utilize high repetition pump laser to make the Stokes wave and pump wave synchronized, as a result, the oscillating Stokes wave and the pump wave could interact with each other and generate narrowband THz wave. In our experiment, owing to the relatively low repetition rate of the pump source (1 kHz), it was not possible to match the cavity round-trip time ( $\sim 1$  ns with the cavity length of 170 mm) with the inter-pulse time of the pump wave ( $\sim 1$  ms with the repetition rate of 1 kHz). It means that the oscillating Stokes wave could not interact with the pump wave. The pump wave and recycling Stokes wave stimulated broadband THz wave independently through TPG process. Therefore, a non-synchronously pumped oscillator was arranged in the experiment. Fig. 2(a) shows the scheme of the terahertz wave generation via Stokes wave recycling process. On the condition of high pump peak power density in the cavity, the primary SPS conversion from the pump to the 1st order Stokes and THz wave plays the main role. Then the oscillation of strong 1st order Stokes wave can benefit the higher order Stokes wave emission and terahertz wave generation. Fig. 2(b) shows the detailed timing sequence of the pump wave passed through the nonlinear crystal, the Stokes wave recycled in the cavity and the THz wave generated in the SPS process. The pump wave transmits through the nonlinear crystal in a single pass. The oscillating Stokes wave stimulated SPS process repeatedly in the cavity. The THz wave could also be generated repeatedly. Thus, the accumulation of these multiple THz wave excitations will bring about the power enhancement of the total THz wave generation. Here, it should be noted that this kind of accumulation is temporal incoherent.

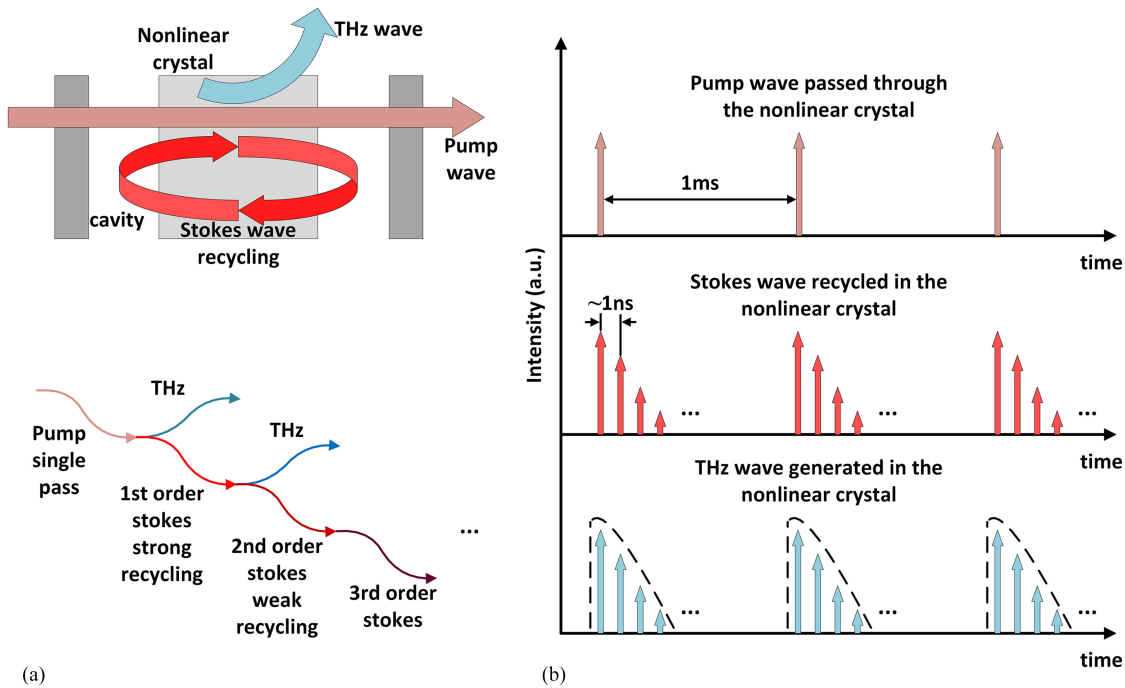


Fig. 2. (a) The scheme of the terahertz wave generation via Stokes wave recycling process. (b) The detailed timing sequence of the pump & Stokes wave transmitted in the nonlinear crystal and the THz wave generated in the stimulated polariton scattering process.

The THz wave, generated by the primary SPS process and the 1st order Stokes wave oscillation induced extra SPS process, can be theoretically demonstrated as

$$f_{THz} = \frac{c}{\lambda_{pump}} - \frac{c}{\lambda_{1st-Stokes}} = \frac{c}{\lambda_{1st-Stokes}} - \frac{c}{\lambda_{2nd-Stokes}} = \dots \quad (1)$$

where  $f_{THz}$  is the frequency of the THz wave,  $c$  is the velocity of light in the vacuum,  $\lambda_{pump}$  refers to the wavelength of the pump,  $\lambda_{1st-Stokes}$  refers to the wavelength of the 1st order Stokes wave and  $\lambda_{2nd-Stokes}$  refers to the wavelength of the 2nd order Stokes wave, respectively. The next higher-order SPS processes are omitted in the equation.

In the primary SPS process, the pump wave with high peak power density leads to the strong and broadband 1st order Stokes wave and THz wave generation. Owing to the oscillating cavity was aligned with part of the 1st order Stokes wave, strong recycling 1st order Stokes wave also stimulates broadband 2nd order Stokes wave and THz wave generation. The other higher order SPS processes are weak on account of the cavity mismatching. Moreover, the angle between the pump and 1st order Stokes wave is smaller than the ones between the pump and higher order Stokes wave. It means that the interaction area between the pump and 1st order Stokes wave is larger than that between the pump and higher order Stokes waves. For this reason, the gain of the THz wave generation mostly comes from the primary SPS process and the 1st order Stokes wave oscillation induced extra SPS process, instead of the interaction between the pump and higher order Stokes waves. That is to say, other higher THz harmonics could be negligible.

To analyze the Stokes wave recycling process in detail, the THz output characteristics were measured as a function of different cavity lengths in the experiment. The oscillating cavity was aligned with part of the 1st order Stokes wave for better recycling. The angle between the pump and the 1st order Stokes wave outside the nonlinear crystal was fixed at 1.3 degrees for stronger THz wave generation. The overall results are demonstrated in Fig. 3. It is clearly shown that under the same pump power, the THz wave generation decreased along with the cavity lengths increasing

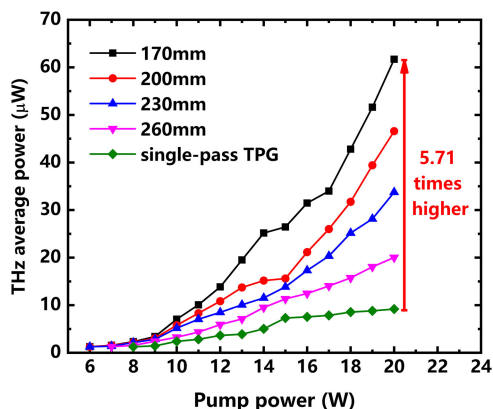


Fig. 3. THz average power as a function of different oscillating cavity lengths.

from 170 mm to 260 mm. Moreover, when the oscillating cavity was removed, namely single-pass TPG, which was equivalent to the condition of infinite cavity length, the lowest power of the THz wave was generated. This phenomenon could be attributed to the change of diffraction loss and angle tolerance in the cavity. According to the classical principle of laser physics [37], the single pass diffraction loss of the oscillating cavity can be theoretically demonstrated as  $\delta_d \approx \frac{L\lambda}{a^2} = \frac{1}{N}$ , where  $L$  is the cavity length,  $\lambda$  is the wavelength of the oscillating wave,  $a$  is the effective aperture radius, and  $N$  is the Fresnel number of the oscillator, respectively. It can be inferred that the longer cavity length resulted in the higher diffraction loss and lower angle tolerance for the 1st order Stokes wave. As a result, under the non-collinear phase-matching condition, the SPS conversion to higher order Stokes wave was weak. Therefore, the enhancement of THz wave generation was also weak. Furthermore, it is obvious that in the condition of the finite cavity length (Stokes wave recycling configuration), Stokes wave recycling could lead to power enhancement of the THz wave generation. However, in the state of infinite cavity length (single-pass TPG), the Stokes wave oscillation process and the enhanced THz wave generation could not exist. From Fig. 3, it is seen that the THz output power from Stokes wave recycling configuration was clearly higher than that from single-pass TPG in the experiment, which was consistent with the theoretical analysis. When the pump power was 20 W and the cavity length was 170 mm, the maximum THz average power was  $61.7 \mu\text{W}$ , and the maximum power conversion efficiency was  $3.085 \times 10^{-6}$ . There was 5.71 times enhancement of the terahertz wave generation compared against the ones from single-pass TPG. In order to avoid the damage to MgO:LN crystal, higher pump power was not attempted. By limitation of the size of the crystal and the optical components, shorter cavity length was not attempted either.

Fig. 4(a) shows the spatial distribution of the pump and Stokes waves (which were visualized by collinear second harmonic generated green light) leaking from the oscillating cavity as a function of the incident pump power from 2 W to 20 W, in the condition of the cavity length was 170 mm and the angle between the pump and 1st order Stokes wave outside the nonlinear crystal was 1.3 degrees. When the incident pump power was 2 W, only the pump wave was visible. As the incident pump power increased, the pump wave was getting much brighter. Till the moment that the incident pump power approached 10 W, different orders of the Stokes waves became clearly visualized, which means that the 1st order Stokes wave was oscillating strong enough and stimulating the higher order Stokes wave in the cavity. Furthermore, when the pump power increased up to 20 W with the pump density of  $5.66 \text{ GW}/\text{cm}^2$ , the anti-Stokes wave emerged, and the pump depletion was 11.2 W in the cavity. It can also verify the extremely strong Stokes waves generation and SPS processes in the cavity.

The spectral output of the pump and Stokes wave under the incident pump power of 20 W was measured, as shown in Fig. 4(b). Since the spatial distribution of the anti-Stokes, pump and Stokes wave were discontinuous, a lens was utilized to focus these beams into the detection fiber of the

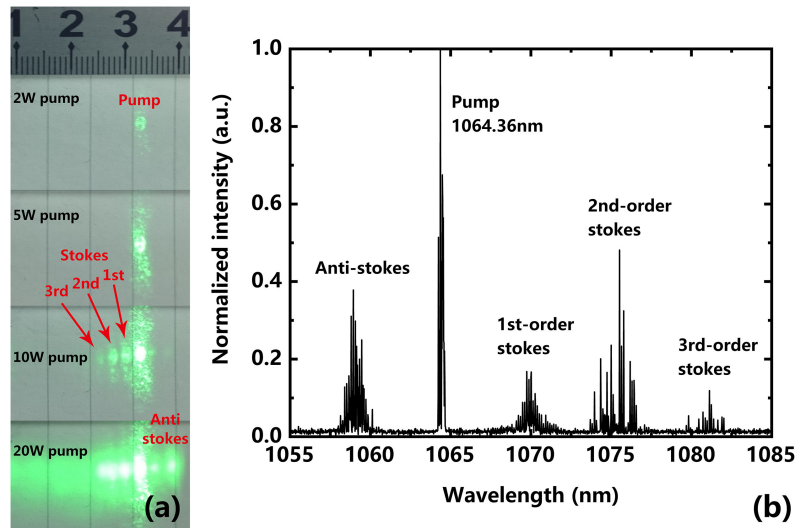


Fig. 4. (a) Spatial distribution of the anti-Stokes, pump and different orders of Stokes waves visualized by collinear second harmonic generated green light. (b) Spectral contents of the anti-Stokes, pump and different orders of Stokes waves.

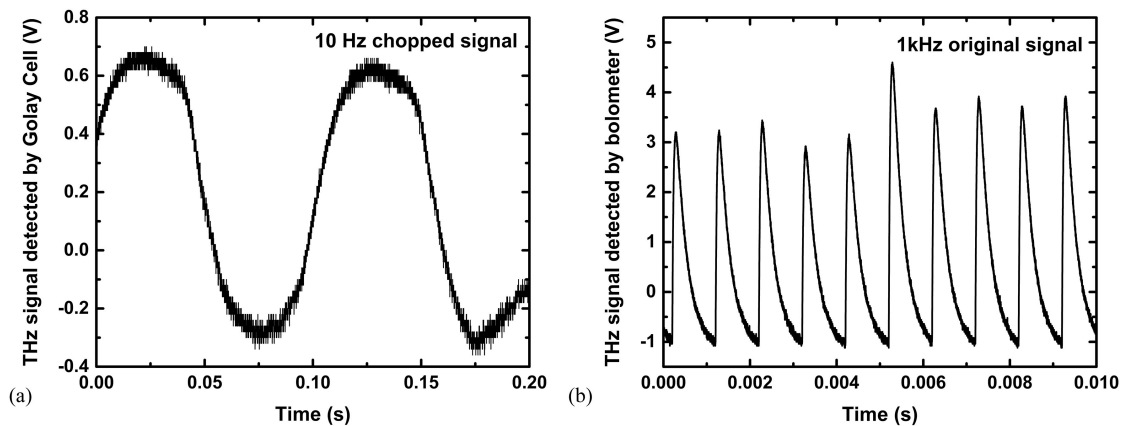


Fig. 5. (a) The THz wave signal detected by Golay Cell under a fixed chopping rate of 10 Hz. (b) The pulse train of the THz wave signal detected by 4K-Silicon bolometer.

optical spectrum analyzer in the experiment. There was one order of broadband anti-Stokes wave (1058.14–1060.12 nm), the narrowband pump wave (1064.36 nm) and three different orders of broadband Stokes waves (1069.08–1071.56 nm, 1073.70–1077.34 nm & 1079.68–1082.02 nm). This spectrum corresponds to the broadband THz-wavelength range of 158.41–241.08  $\mu\text{m}$  (1.24–1.89 THz). It should be noted that this kind of focusing measurement could lead to different coupling efficiency between different waves, thus the normalized intensity between different spectral lines in Fig. 4(b) are incomparable. The cavity in our experiment was not synchronized for the pump and Stokes wave. As a result, the oscillating Stokes wave and the pump wave could not interact with each other. The cavity was only for Stokes wave recycling rather than THz wave frequency tuning. The pump wave and recycling Stokes wave stimulated broadband THz wave independently through TPG process. Overall, the narrowband pump wave with high peak power density led to the strong and broadband 1st order Stokes wave and THz wave generation through SPS process. Then the strong 1st order Stokes wave was recycling in the oscillating cavity. And the

broadband 1st order Stokes wave stimulated the wider broadband 2nd order Stokes wave and THz wave. At the same time, the anti-Stokes and the higher order Stokes wave were also stimulated as a result of the strong SPS process.

Fig. 5(a) shows the THz wave signal detected by Golay Cell under a fixed chopping rate of 10 Hz. Considering that the time constant of Golay Cell is always larger than 10 ms, we have to utilize the chopper combined with the Golay Cell for measurement when the repetition rate of the detected signal is larger than 100 Hz. This kind of chopped THz wave signal was almost the same as the chopped signal of the continuous THz wave, which differs from the conventional pulsed ones. It can be deduced that the calculation of the THz wave average power was reliable in our experiment. In addition, considering the time constant of 4K-Silicon bolometer is about 1 ms, it helped us obtain the pulse train of the THz wave signal, as shown in Fig. 5(b). The THz wave signal of 1 kHz repetition rate can be well observed.

#### 4. Conclusion

In conclusion, the enhancement of the terahertz wave generation via Stokes wave recycling based on non-synchronously picosecond pulse pump has been demonstrated in this paper. The process of enhanced terahertz wave generation via Stokes wave recycling has been investigated theoretically. High pump peak power density led to powerful primary SPS conversion from the pump to the 1st order Stokes wave. The oscillation of strong 1st order Stokes wave benefitted the higher order Stokes wave emission and the power enhancement of terahertz wave generation. The experimental results show the maximum enhancement ratio of the THz power was 5.71 times compared with the conventional single-pass TPG configuration. This kind of simple configuration may lead to improvements in robust, reliable, compact and cost-effective THz sources with broadband and sufficient output in future researches.

---

#### References

- [1] P. H. Siegel, "Terahertz technology," *IEEE Trans. Microw. Theory Techn.*, vol. 50, no. 3, pp. 910–928, Mar. 2002.
- [2] M. Tonouchi, "Cutting-edge terahertz technology," *Nature Photon.*, vol. 1, no. 2, pp. 97–105, 2007.
- [3] P. E. Powers, *Fundamentals of Nonlinear Optics*, Boca Raton, FL, USA: CRC Press, 2011.
- [4] J. M. Yarborough, S. S. Sussman, H. E. Puthoff, R. H. Pantell, and B. C. Johnson, "Efficient, tunable optical emission from LiNbO<sub>3</sub> without a resonator," *Appl. Phys. Lett.*, vol. 15, no. 3, pp. 102–105, 1969.
- [5] B. C. Johnson, H. E. Puthoff, J. Soohoo, and S. S. Sussman, "Power and linewidth of tunable stimulated far-infrared emission in LiNbO<sub>3</sub>," *Appl. Phys. Lett.*, vol. 18, no. 5, pp. 181–183, 1971.
- [6] M. A. Piestrup, R. N. Fleming, and R. H. Pantell, "Continuously tunable submillimeter wave source," *Appl. Phys. Lett.*, vol. 26, no. 8, pp. 418–421, 1975.
- [7] J. Shikata, K. Kawase, M. Sato, T. Taniuchi, and H. Ito, "Characteristics of coherent terahertz wave generation from LiNbO<sub>3</sub> optical parametric oscillator," *Electr. Commun. Jpn.*, vol. 82, pp. 46–53, 1999.
- [8] K. Imai, K. Kawase, and H. Ito, "A frequency-agile terahertz-wave parametric oscillator," *Opt. Exp.*, vol. 8, no. 13, pp. 699–704, 2001.
- [9] K. Kawase, J. I. Shikata, and H. Ito, "Terahertz wave parametric source," *J. Phys. D, Appl. Phys.*, vol. 35, no. 3, pp. R1–R14, 2002.
- [10] S. Hayashi *et al.*, "Tunability enhancement of a terahertz-wave parametric generator pumped by a microchip Nd:YAG laser," *Appl. Opt.*, vol. 48, no. 15, pp. 2899–2902, 2009.
- [11] T. Ikari, X. Zhang, H. Minamide, and H. Ito, "THz-wave parametric oscillator with a surface-emitted configuration," *Opt. Exp.*, vol. 14, pp. 1604–1610, 2006.
- [12] W. Wang *et al.*, "Terahertz parametric oscillator based on KTiOPO<sub>4</sub> crystal," *Opt. Lett.*, vol. 39, no. 13, pp. 3706–3709, 2014.
- [13] W. Wang *et al.*, "THz-wave generation via stimulated polariton scattering in KTiOAsO<sub>4</sub> crystal," *Opt. Exp.*, vol. 22, no. 14, pp. 17092–17098, 2014.
- [14] C. Yan *et al.*, "Green laser induced terahertz tuning range expanding in KTiOPO<sub>4</sub> terahertz parametric oscillator," *Appl. Phys. Lett.*, vol. 108, no. 1, pp. 910–928, 2016.
- [15] Z. Yang *et al.*, "High-energy terahertz wave parametric oscillator with a surface-emitted ring-cavity configuration," *Opt. Lett.*, vol. 41, pp. 2262–2265, 2016.
- [16] D. J. M. Stoithard *et al.*, "Line-narrowed, compact, and coherent source of widely tunable terahertz radiation," *Appl. Phys. Lett.*, vol. 92, no. 14, 2008, Art. no. 141105.
- [17] C. L. Thomson and M. H. Dunn, "Observation of a cascaded process in intracavity terahertz optical parametric oscillators based on lithium niobate," *Opt. Exp.*, vol. 21, pp. 17647–17658, 2013.



- [18] A. J. Lee and H. Pask, "Continuous wave, frequency-tunable terahertz laser radiation generated via stimulated polariton scattering," *Opt. Lett.*, vol. 39, pp. 442–445, 2014.
- [19] A. Lee and Helen M. Pask, "Cascaded stimulated polariton scattering in a Mg:LiNbO<sub>3</sub> terahertz laser," *Opt. Exp.*, vol. 23, pp. 8687–8698, 2015.
- [20] T. Ortega, H. Pask, D. Spence, and A. Lee, "Stimulated polariton scattering in an intracavity RbTiOPO<sub>4</sub> crystal generating frequency-tunable THz output," *Opt. Exp.*, vol. 24, pp. 10254–10264, 2016.
- [21] A. Lee, D. Spence, and H. Pask, "Tunable THz polariton laser based on 1342 nm wavelength for enhanced terahertz wave extraction," *Opt. Lett.*, vol. 42, pp. 2691–2694, 2017.
- [22] T. Ortega, H. Pask, D. Spence, and A. Lee, "Tunable 3–6 THz polariton laser exceeding 0.1 mW average output power based on crystalline RbTiOPO<sub>4</sub>," *IEEE J. Sel. Topics Quantum Electron.*, vol. 24, no. 5, Sep./Oct. 2018, Art. no. 5100806.
- [23] K. Nawata *et al.*, "Effective terahertz wave parametric generation depending on the pump pulse width using a LiNbO<sub>3</sub> crystal," *IEEE Trans. Terahertz Sci. Technol.*, vol. 7, no. 5, pp. 617–620, Sep. 2017.
- [24] D. Walsh, D. J. M. Stothard, T. J. Edwards, P. G. Browne, C. F. Rae, and M. H. Dunn, "Injection-seeded intracavity terahertz optical parametric oscillator," *J. Opt. Soc. Amer. B*, vol. 26, pp. 1196–1202, 2009.
- [25] M. Wu *et al.*, "Terahertz parametric generation and amplification from potassium titanyl phosphate in comparison with lithium niobate and lithium tantalate," *Opt. Exp.*, vol. 24, pp. 25964–25973, 2016.
- [26] S. Hayashi, K. Nawata, T. Taira, J. Shikata, K. Kawase, and H. Minamide, "Ultrabright continuously tunable terahertz-wave generation at room temperature," *Sci. Rep.*, vol. 4, no. 5, pp. 2253–2253, 2014.
- [27] G. Tang *et al.*, "Energy scaling of terahertz-wave parametric sources," *Opt. Exp.*, vol. 23, pp. 4144–4152, 2015.
- [28] K. Murate, S. Hayashi, and K. Kawase, "Expansion of the tuning range of injection-seeded terahertz-wave parametric generator up to 5 THz," *Appl. Phys. Exp.*, vol. 9, no. 8, 2016, Art. no. 082401.
- [29] S. Hayashi, K. Nawata, Y. Takida, Y. Tokizane, K. Kawase, and H. Minamide, "High-brightness continuously tunable narrowband subterahertz wave generation," *IEEE Trans. Terahertz Sci. Technol.*, vol. 6, no. 6, pp. 858–861, Nov. 2016.
- [30] Y. Chiu, T. Wang, G. Zhao, and Y. Huang, "Discovery of high-gain stimulated polariton scattering near 4 THz from lithium niobate," *Opt. Lett.*, vol. 42, pp. 4897–4900, 2017.
- [31] Y. Moriguchi *et al.*, "High-average and high-peak output-power terahertz-wave generation by optical parametric down-conversion in MgO: LiNbO<sub>3</sub>," *Appl. Phys. Lett.*, vol. 113, no. 12, 2018, Art. no. 121103.
- [32] Y. Takida, S. Maeda, T. Ohira, H. Kumagai, and S. Nashima, "Noncascading THz-wave parametric oscillator synchronously pumped by mode-locked picosecond Ti: Sapphire laser in doubly-resonant external cavity," *Opt. Commun.*, vol. 284, no. 19, pp. 4663–4666, 2011.
- [33] Y. Takida, T. Ohira, Y. Tadokoro, and H. Kumagai, "Tunable picosecond terahertz-wave parametric oscillators based on noncollinear pump-enhanced signal-resonant cavity," *IEEE J. Sel. Topics Quantum Electron.*, vol. 19, no. 1, Jan./Feb. 2013, Art. no. 8500307.
- [34] A. M. Warrier, R. Li, J. Lin, A. Lee, H. Pask, and D. Spence, "Tunable terahertz generation in the picosecond regime from the stimulated polariton scattering in a LiNbO<sub>3</sub> crystal," *Opt. Lett.*, vol. 41, pp. 4409–4412, 2016.
- [35] J. Liu, W. Wang, Z. Wang, Z. Lv, Z. Zhang, and Z. Wei, "Diode-pumped high energy and high average power all-solid-state picosecond amplifier systems," *Appl. Sci.*, vol. 5, no. 4, pp. 1590–1602, 2015.
- [36] T. Ikari, X. Zhang, H. Minamide, and H. Ito, "THz-wave parametric oscillator with a surface-emitted configuration," *Opt. Exp.*, vol. 14, no. 4, pp. 1604–1610, 2006.
- [37] A. E. Siegman, *Lasers*, Sausalito, CA, USA: University Science Books, 1986.